TABLE 1.—Body weight, brain weight, and cerebellum weight.

	PND7				PND14				PND21			
	Control		Cyclopamine		Control		Cyclopamine		Control		Cyclopamine	
	Wild	Ptch1	Wild	Ptch1	Wild	Ptch1	Wild	Ptch1	Wild	Ptch1	Wild	Ptch1
n	8	12	7	17	6	12	9	9	6	17	7	18
Body weight (g)	4.4 ± 0.9	3.9 ± 0.8	3.8 ± 0.2	3.6 ± 0.6	6.6 ± 0.4	6.5 ± 1.0	6.1 ± 1.6	6.5 ± 1.3	9.4 ± 1.5	9.7 ± 1.5	9.7 ± 1.7	9.2 ± 1.7
Brain weight (mg)	243 ± 17	256 ± 12	228 ± 11	238 ± 19**	341 ± 16	379 ± 19	324 ± 26	363 ± 21	417 ± 29	453 ± 18	366 ± 16**	410 ± 25**
Cerebellum weight (mg)	64 ± 6	74 ± 6	61 ± 4	66 ± 6**	94 ± 5	108 ± 5	90 ± 8	106 ± 11	115 ± 8	133 ± 9	102 ± 3**	119 ± 10**

Note. PND = postnatal day; Ptch1 = patched1.

**Significantly different from control group at $p < .01$.

Glostrup, Denmark) as a proliferation marker, monoclonal rabbit anti-cleaved caspase-3 (Clone 5A1E, Cell Signaling, Danvers, MA) as an apoptotic marker, and monoclonal mouse anti-NeuN (Clone A60, Millipore, Billerica, MA) as a mature granule cell marker. A streptavidin–biotin labeling method was performed with the anti-Ki-67 antibody using a polyclonal rabbit anti-rat biotinylated IgG (Dako Cytomation) and streptavidin-conjugated horseradish peroxidase (Dako Cytomation). A polymer labeling method was performed for the anti-cleaved caspase-3 and anti-NeuN antibodies using the Histofine Simple Stain kit (Nichirei Biosciences Inc., Tokyo, Japan). The immunoreactions were visualized by a peroxidase-diaminobenzidine reaction. The sections were then lightly counterstained with hematoxylin.

Morphometric Assessment

For total area of proliferative lesions in the cerebellum, photomicrographs of the cerebellar sections were taken with a digital camera attached to a microscope (DP71, Olympus Corp., Tokyo, Japan), then measurements were made using image analysis software (WinROOF, Version 5.7.1, Mitani Corp., Tokyo, Japan). The total area of proliferating cells in the cerebellum, including Ki-67-positive foci and MBs (Matsuo et al. 2013), was measured as the Ki-67-positive cell area, and the ratio of the total proliferating area to the total area of the cerebellum was calculated for Ptch1 mice at PND21 and W12. For width of the EGL and outer layer of EGL, slides stained with Ki-67 antibody were scanned using Aperio ScanScope (Aperio, Vista, CA), then measurements were made using image analysis software (ImageScope, Version 10.2.1.2315, Aperio, Vista, CA). The width of the EGL and the outer layer of the EGL of each mouse at PND7 was determined by 5 measurements selected at random from the 3rd cerebellar lobule.

Statistical Analysis

For body weight, organ weight, proliferating area of the cerebellum, and width of the EGL and outer layer of the EGL, values of cyclopamine-treated mice at each time point were compared with the corresponding vehicle controls using the Student's *t*-test following a test for equal variance. Incidence of histopathological findings was compared using Fisher's exact probability test.

Results

General Remarks

There were no significant differences in body weight at each time point when control and cyclopamine-treated mice were compared by genotype (Table 1). All wild-type and Ptch1 mice survived the duration of the experimental period. In addition, no clinical signs of tumor progression were detected in either genotype with or without cyclopamine treatment up to 12 weeks of age.

Absolute weights of the whole brain and cerebellum significantly decreased in Ptch1 mice in the cyclopamine group at PND7, and in both genotypes in the cyclopamine group at PND21 compared to the control group (Table 1).

Effect of Cyclopamine on Proliferative Lesions in the Cerebellum of Ptch1 Mice

No proliferative lesions were detected in the cerebellum of wild-type mice at any time point (Figure 1). The incidence of lesions was calculated as the number of animals that had a specific lesion (e.g., Ki-67-positive foci) in the cerebellum relative to the total number of animals examined (Figures 2 and 3). At PND14, the incidence of thickened areas in the EGL was significantly decreased in the cyclopamine group in Ptch1 mice (Figure 3). In addition, the incidence of Ki-67-positive foci and small MBs was significantly decreased in the cyclopamine group in Ptch1 mice at PND21 (Figure 3). The incidence of proliferative lesions in the cerebellum of the cyclopamine group in Ptch1 mice at W12 was decreased but was not statistically significant (Figure 3).

Immunohistochemistry for Ki-67 revealed that the total area of proliferative lesions in the cerebellum was significantly decreased in the cyclopamine group in Ptch1 mice at PND21 (Figure 4). Additionally, a decreasing trend in the total area of proliferative lesions at W12 was observed (Figure 4).

Effects of Cyclopamine on Cerebellar Development

To examine the specific inhibitory effects of cyclopamine on the development of MBs and their preneoplastic lesions, we also performed histopathology of the cerebellum of control and cyclopamine-treated mice during the early developmental period of the cerebellum at PND7. The width of the EGL was noticeably thinned in the cyclopamine group compared to the control group regardless of genotype at PND7 (Figures 5A and 6, pictures of wild-type mice not shown). The thinning of the EGL was mainly observed in lobules 2 through 4/5 of the cerebellum and was obscure in lobules 6 through 10. Immunohistochemical staining with the anti-Ki-67 antibody revealed that the outer layer of the EGL, which is composed of proliferating GCPs, was also thinned in Ptch1 mice in the cyclopamine group (Figures 5B and 6, pictures of wild-type mice not shown). Decreasing trend was observed in the outer layer of the EGL in cyclopamine group of wild-type mice (Figure 5B). There was no increase in cleaved caspase-3-positive apoptotic cells in the EGL of the cyclopamine group compared to the control group (Figure 6).

Histopathological examination revealed that cells morphologically resembling nuclei of the internal granular layer were distributed parallel to the Purkinje cell layer in the deep molecular layer of the cyclopamine group at PND14 and 21 regardless of genotype (Figure 7). These nuclei were strongly labeled for NeuN (Figure 8). These findings were also present in the cerebellum of the cyclopamine-treated group at W12 (Figures 7 and 8). Furthermore, misalignment of the Purkinje cells was

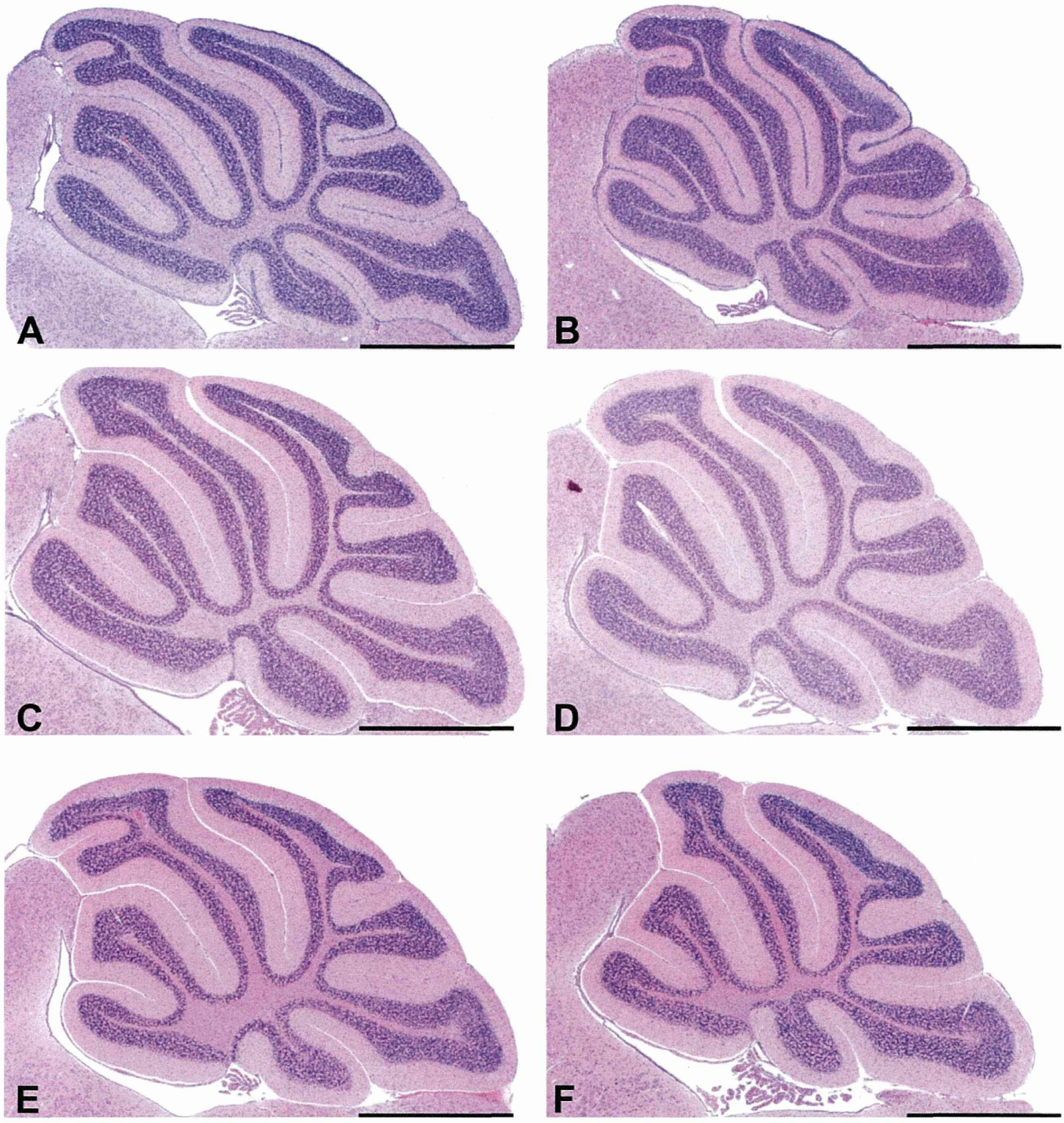

FIGURE 1.—Representative images of the cerebellum from control (left) and cyclopamine-treated (right) wild-type mice at PND14 (A, B), 21 (C, D) and W12 (E, F). No proliferative lesions were detected in the cerebellum of wild-type mice at any time point. Scale bar: 1000 μm.
Note. PND = postnatal day; W12 = postnatal week 12.

scattered in the cyclopamine group at PND14 and 21, and this finding was observed up to W12 (Figure 9). These findings were mainly observed in lobules 2 through 4/5 of the cerebellum and were obscure in lobules 6 through 10 in both genotypes (pictures of wild type not shown).

DISCUSSION

Currently, human MBs have been classified into at least 4 distinct subtypes by molecular studies (Ellison et al. 2011; Northcott et al. 2011; Jones et al. 2012; Kool et al. 2012; Kawauchi et al. 2012). MBs of the Shh subgroup result from

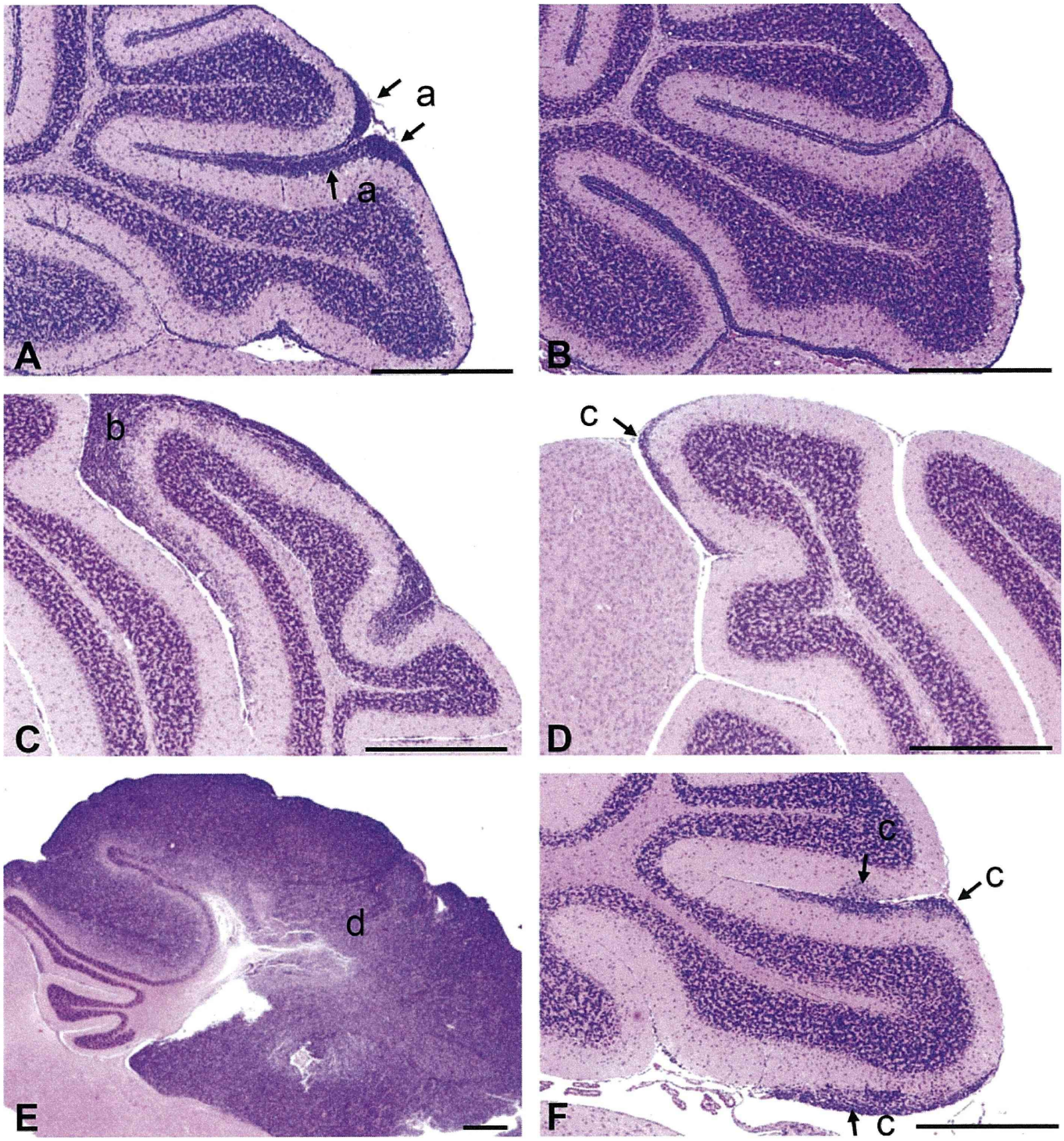

FIGURE 2.—Representative proliferative lesions in the cerebellum of control (left) and cyclopamine-treated (right) Ptch1 mice at PND14 (A, B), 21 (C, D) and W12 (E, F). Proliferative lesions in the cerebellum were classified into the following 4 types: (a) thickened area of the EGL, (b) small MB, (c) Ki-67 positive focus, and (d) large MB. Scale bar: 500 μm.
Note. PND = postnatal day; W12 = postnatal week 12; Ptch1 = patched1; EGL = external granular layer; MB = medulloblastoma.

inactivating mutations of PTCH1 or mutations of other components of the Shh signaling pathway (Kawauchi et al. 2012). It is known that the expression of Gli1 is increased in MBs of Ptch1 mice compared to expression in the normal cerebellum, suggesting activation of the Shh signaling pathway in these tumors (Raffel 2004). Recently, many Shh pathway inhibitors such as cyclopamine, HhAntag, GDC-0449, and IPI-926 have been identified and tested in preclinical and clinical studies

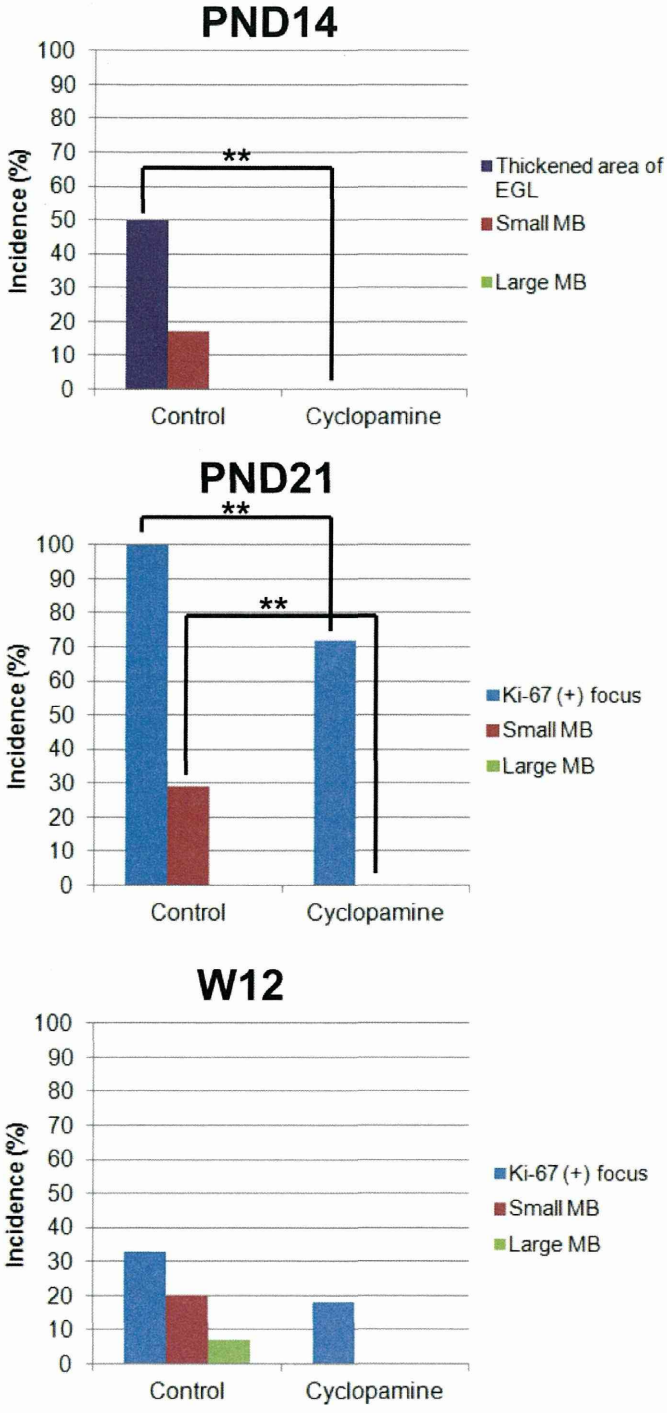

FIGURE 3.—Incidence of proliferative lesions in the cerebellum of control and cyclopamine-treated Ptch1 mice at PND14, 21, and W12. **Significantly different from control group; $p < .01$.
Note. PND = postnatal day; W12 = postnatal week 12; Ptch1 = patched1.

targeting MB and other Shh pathway–activated tumors (Gajjar et al. 2013; Gupta, Takebe, and Lorusso 2010; Lee et al. 2012; Low and Sauvage 2010; Scales and Sauvage 2009). The Ptch1 mouse has been used in various studies as an Shh-subtype MB model (Behesti and Marino 2009; Sanchez and Ruiz i Altaba 2005).

During postnatal cerebellar development in mice, proliferation of GCPs occurs throughout the 2 weeks after birth and GCPs migrate into the internal granular layer by PND21 (Behesti and Marino 2009; Haldipur et al. 2012; Vaillant and Monard 2009). During postnatal cerebellar development, Ptch1 mice show a high incidence of preneoplastic MB lesions such as thickened areas in the EGL and Ki-67 positive foci (Matsuo et al. 2013). The present study clearly showed that postnatal exposure to cyclopamine inhibited the occurrence of preneoplastic MB lesions and small MBs in Ptch1 mice up to 1 week after the treatment period. Concurrently, the reduction in the total area of proliferative lesions in the cyclopamine group indicated that cyclopamine treatment inhibited not only the development of preneoplastic lesions but also the expansion of these lesions. Furthermore, the inhibitory potential persisted for 2 months after treatment.

During normal cerebellar development, Shh is an important signal that regulates GCP proliferation in the EGL (Haldipur et al. 2012; Lewis et al. 2004; Vaillant and Monard 2009; Wallace 1999). GCPs express Ptch1, the receptor for Shh, and proliferate in response to Shh secreted by the Purkinje cells (Haldipur et al. 2012; Lewis et al. 2004; Vaillant and Monard 2009). Examination of the cerebellum at the peak period of GCP proliferation, PND7, provided evidence that the inhibitory effect of cyclopamine on GCP proliferation might be related to the thinning of the EGL, a place of occurrence of preneoplastic cells of MBs, in wild-type and Ptch1 mice. Immunohistochemistry indicated that thinning of the EGL was associated with decreased proliferative activity rather than increased apoptosis of GCPs by cyclopamine. In this study, at PND7, the outcome of GCPs treated with cyclopamine was consistent with GCPs treated with neutralizing anti-Shh antibodies in neonatal mice (Wallace 1999). It is known that cyclopamine inhibits the growth of cultured MB cells and allografts by inhibiting Smo (Berman et al. 2002; Dahmane et al. 2001). Furthermore, it has been reported that cyclopamine treatment inhibited MB growth *in vivo* using $Ptc1^{+/-}/p53^{-/-}$ mice and genetically engineered mice overexpressing hepatocyte growth factor (HGF) and Shh by inducing a potent apoptotic death response in tumor cells and by a suppressive effect on proliferation (Coon et al. 2010; Sanchez and Ruiz i Altaba 2005). In addition, another Smo-binding antagonist, HhAntag, completely eliminated MBs by blocking tumor cell proliferation and stimulating apoptosis (Gupta, Takebe, and Lorusso 2010; Romer et al. 2004). Taken together, the decreased proliferative activity observed in cyclopamine-treated mice in this study is thought to be attributed to the inhibition of Smo and downstream signals. Since Ptch1 haploinsufficiency alone is considered to be insufficient for tumor induction, additional genetic lesions are required for tumorigenesis (Wetmore, Eberhart, and Curran 2000; Corcoran and Scott 2001). Our data suggest that cyclopamine treatment during cerebellar development reduced production of cells that will give rise to MBs and the subsequent chances for additional mutations to occur in those cells, by decreasing proliferation of GCPs and preneoplastic cells.

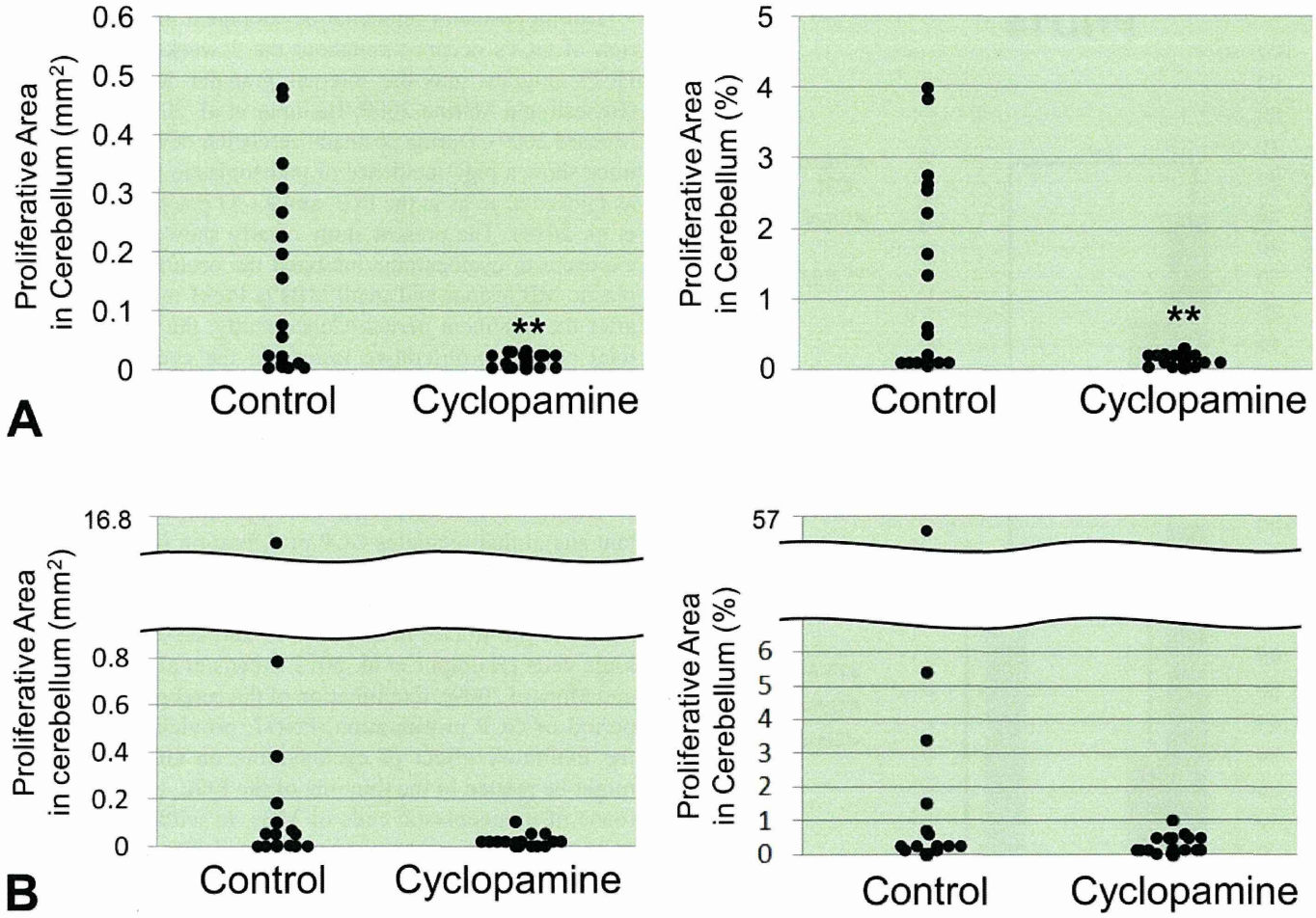

FIGURE 4.—Total area of proliferative lesions in the cerebellum of control and cyclopamine-treated Ptch1 mice at PND21 (A) and W12 (B). The total area of the proliferative lesions was calculated for each animal as the sum of areas of the Ki-67 positive foci and MBs observed in a cerebellum slide stained for Ki-67. **Significantly different from the control group; $p < .01$.
Note. PND = postnatal day; W12 = postnatal week 12; Ptch1 = patched1; MB = medulloblastoma.

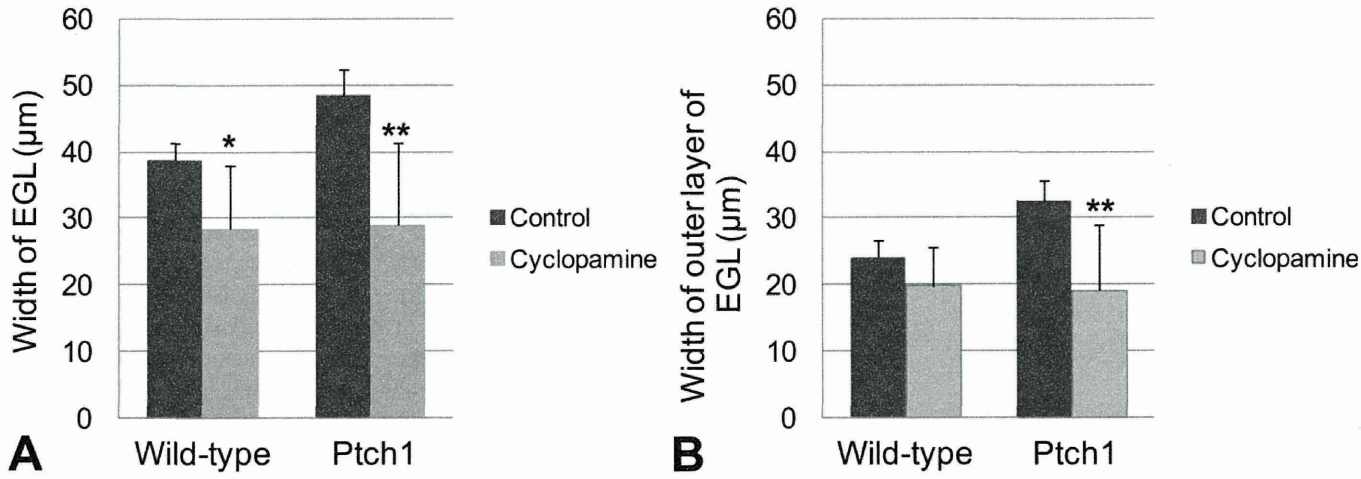

FIGURE 5.—The width of the EGL (A) and the outer layer of the EGL (B) of control and cyclopamine-treated Ptch1 and wild-type mice at PND7. *, **Significantly different from the control group at $p < .05$ and $p < .01$, respectively.
Note. PND = postnatal day; Ptch1 = patched1; EGL = external granular layer.

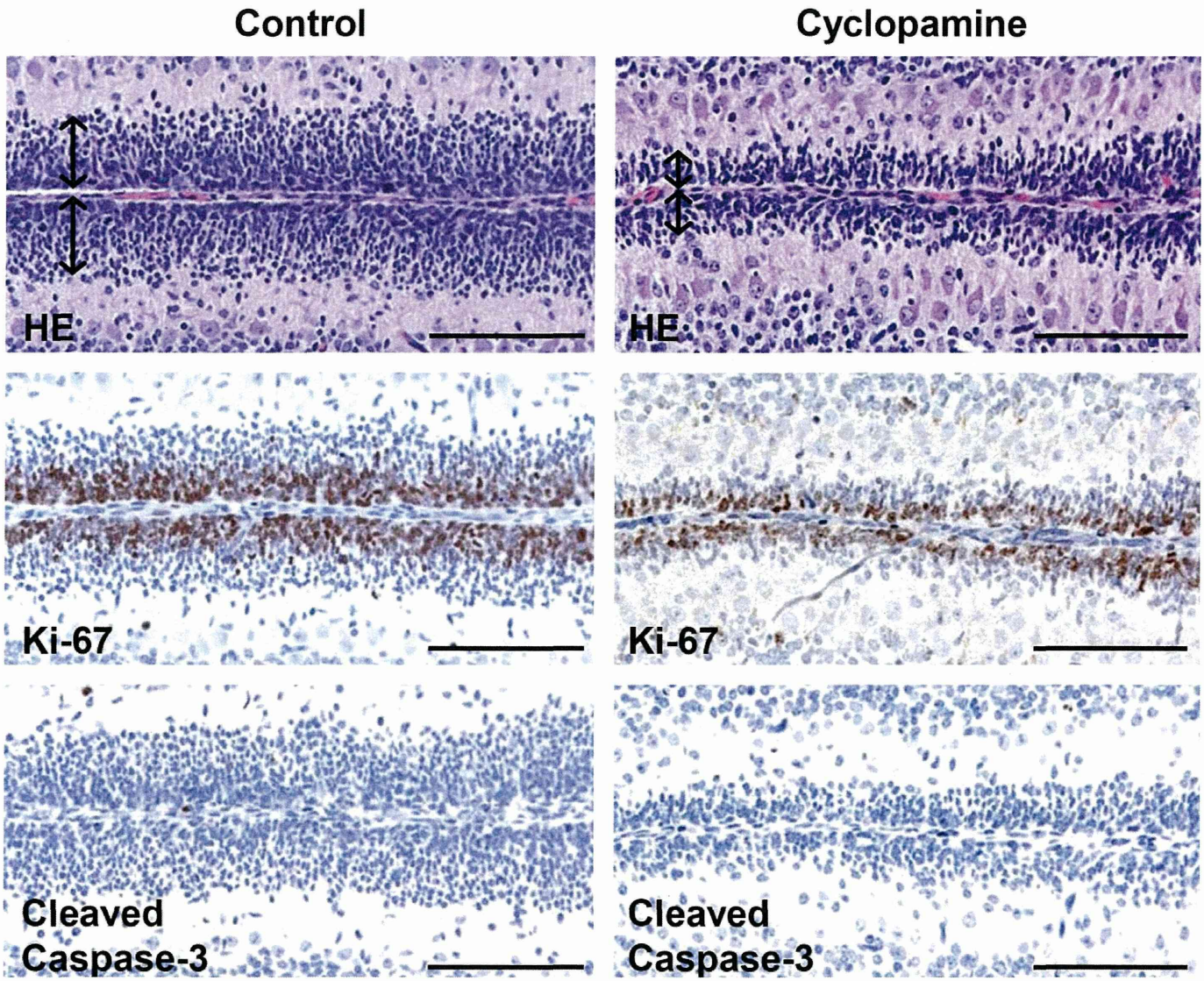

FIGURE 6.—Histopathology of the cerebellum of control (left column) and cyclopamine-treated (right column) Ptch1 mice at PND7. The EGL (arrows) was thinned in the cyclopamine group (HE, top of right column). Thinning of the Ki-67 positive layer in the EGL was also observed in the cyclopamine group (Ki-67 staining, middle of right column). There was no difference in the number of apoptotic cells in the EGL of the cyclopamine group (cleaved caspase-3 staining, bottom of right column) compared to controls. Scale bar: 100 μm.
Note. PND = postnatal day; Ptch1 = patched1; EGL = external granular layer; HE = hematoxylin and eosin.

Cerebellum volume dramatically increases during neonatal development (Lewis et al. 2004). This increase in size is predominantly due to rapid proliferation and expansion of granular cells, which are the most abundant neuronal population in the mature brain (Lewis et al. 2004). In addition, it is known that Shh is required for proliferation of precursor cells of the cerebral neocortex and tectum in postnatal mice in addition to the cerebellum (Dahmane et al. 2001; Stecca and Ruiz i Altaba 2002). Therefore, the decrease in cerebellum weight in the cyclopamine-treated group was considered to be a result of the decreased proliferation of GCPs in the EGL. Furthermore, this suggests that inhibition of Shh signaling by cyclopamine has a similar effect on postnatal cerebral development, as it does on cerebellar development and causes a decrease in overall brain weight.

NeuN-positive granular cells in the deep molecular layer of the cyclopamine-treated group may undergo precocious maturation during their migration to the internal granular layer. Abnormal Purkinje cells similar to those observed in this study have also been reported in Shh-deficient mice and were thought to be a secondary effect due to loss of GCPs (Lewis et al. 2004). In our study, the thinning of the EGL, the presence of ectopic NeuN-positive granular cells, and the misalignment of Purkinje cells are all thought to be caused by cyclopamine treatment and are related to each other because these lesions shared a common location in the cerebellum. Also, the presence of these lesions at W12 indicated that the effects of cyclopamine persisted after the completion of cerebellar development.

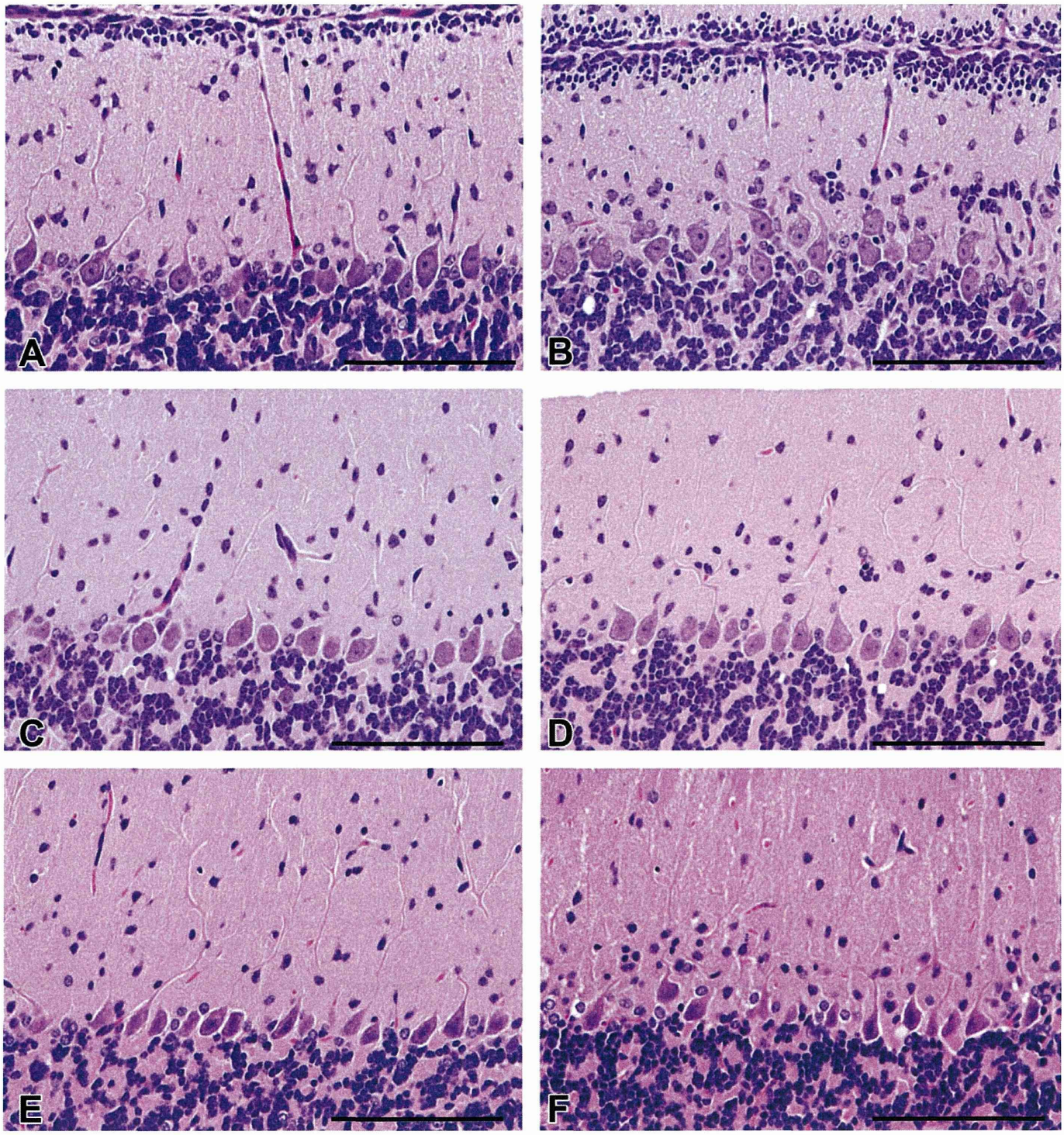

FIGURE 7.—Histopathological findings observed in the molecular layer of the cerebellum from control (left column) and cyclopamine-treated (right column) Ptch1 mice at PND14 (A and B), 21 (C and D), and W12 (E and F) (HE). Granular cells, which resemble cells of the internal granular layer, were distributed parallel to the Purkinje cell layer in the deeper molecular layer of cyclopamine-treated Ptch1 mice at PND14 (B), 21 (D), and W12 (F). Scale bar: 100 μm.
Note. PND = postnatal day; W12 = postnatal week 12; Ptch1 = patched1; HE = hematoxylin and eosin.

Whereas our previous study revealed that more than half of the Ki-67-positive foci and small MBs were located in lobules 6 through 10 of the cerebellum (Matsuo et al. 2013), in the present study the inhibitory effect of cyclopamine was observed mainly in lobules 2 through 4/5 of the cerebellum at PND7. The differences in regions that were highly affected by cyclopamine treatment during the developmental period and the common site of MB

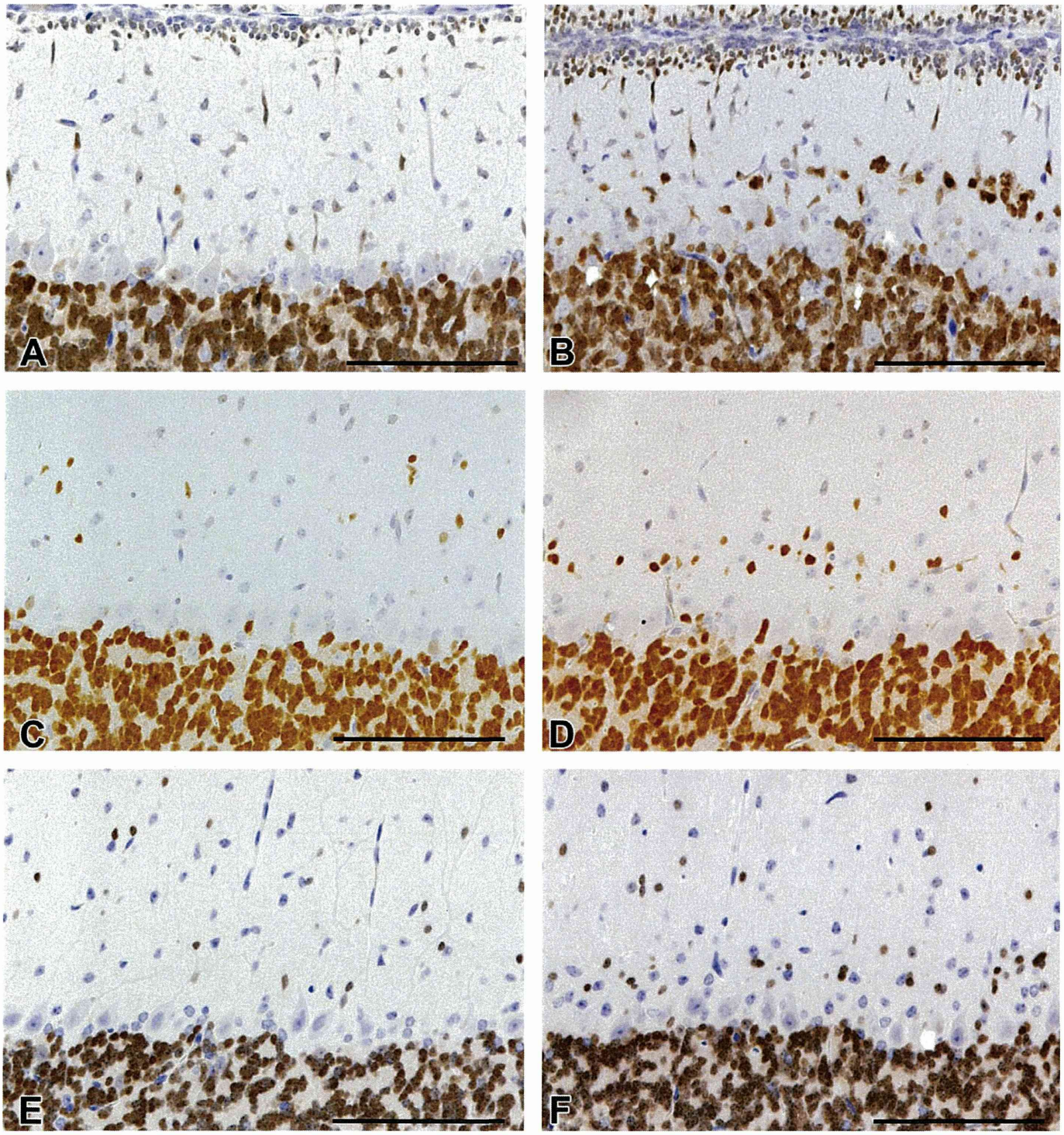

FIGURE 8.—Immunohistochemistry for NeuN of the cerebellum from control (left column) and cyclopamine-treated (right column) Ptch1 mice at PND14 (A and B), 21 (C and D), and W12 (E and F). Granular cells of the internal granular layer were strongly positive for NeuN in all animals. In addition, NeuN positive cells were distributed parallel to the Purkinje cell layer in the deeper molecular layer of cyclopamine-treated Ptch1 mice at PND14 (B), 21 (D), and W12 (F). Scale bar: 100 μm.
Note. PND = postnatal day; Ptch1 = patched1; W12 = postnatal week 12.

formation in the cerebellum of Ptch1 mice might result from incomplete inhibitory effects on the MBs. Another possible explanation for these differences is the potency of cyclopamine, which has recently been shown to be only a moderate inhibitor of hedgehog (Hh) target gene transcription compared to several other more potent synthetic inhibitors of Hh signaling. However, given that cyclopamine was the first Hh signaling inhibitor available, it has been used in many *in vitro* and *in*

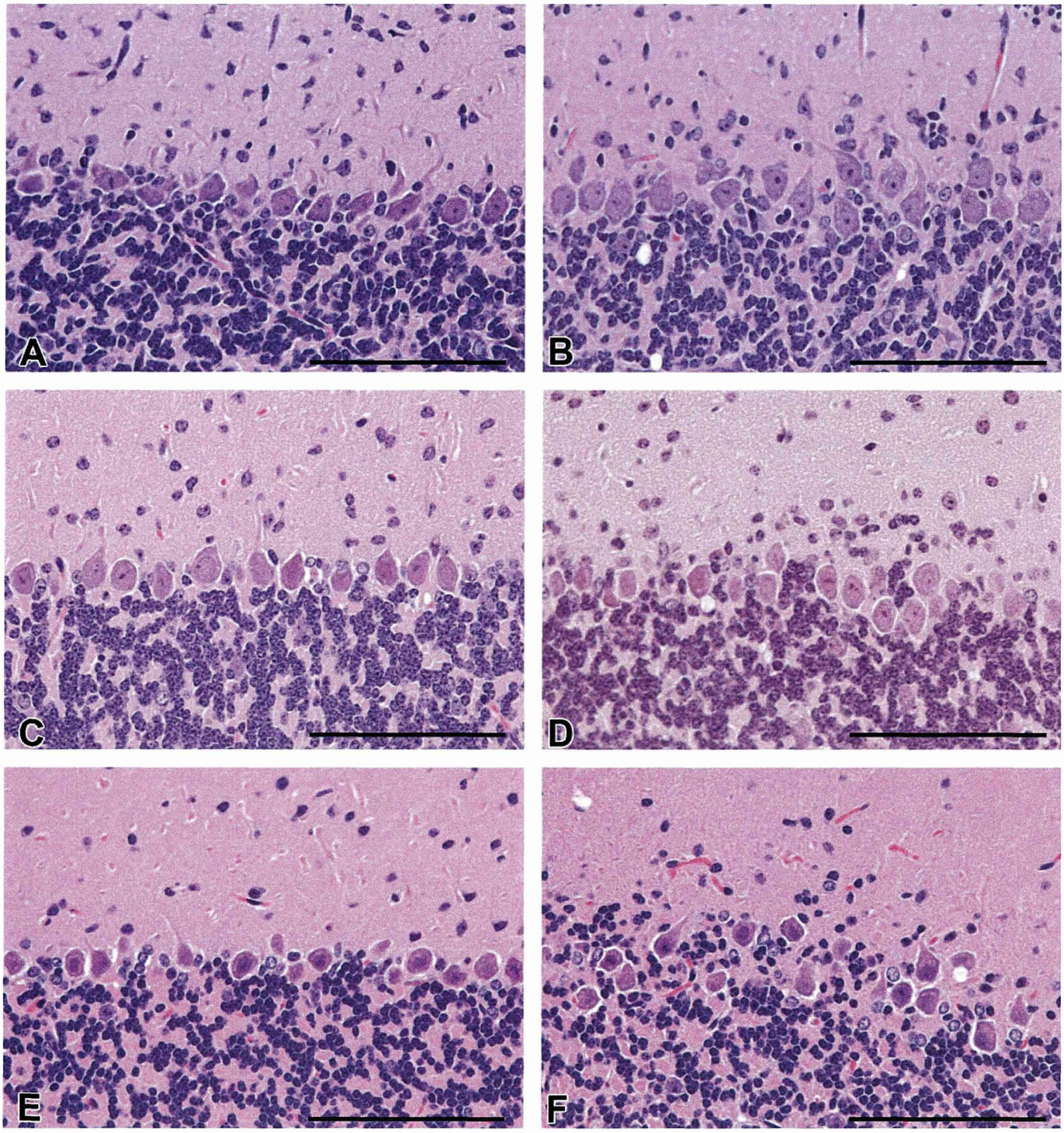

FIGURE 9.—Histopathological findings observed in the Purkinje cell layer of the cerebellum from control (left column) and cyclopamine-treated (right column) Ptch1 mice at PND14 (A and B), 21 (C and D), and W12 (E and F) (HE). Misalignment of Purkinje cells was observed in the cyclopamine group at PND14 (B), 21 (D), and W12 (F). Scale bar: 100 μm.
Note. PND = postnatal day; Ptch1 = patched1; W12 = postnatal week 12; HE = hematoxylin and eosin.

vivo studies (Heretsch et al. 2010a and b; Fan et al. 2011; Gupta, Takebe, and Lorusso 2010; Scales and Sauvage 2009).

In summary, cyclopamine treatment during cerebellar development has inhibitory effect on proliferation of the EGL and development of MB and preneoplastic lesions in Ptch1 mice, and tendency to inhibit these proliferative lesions is prolonged after treatment. This demonstrates that the Ptch1 mouse is a good model for studying the modifying effects of chemical exposure on MB development during the developmental period.